Ingeniería
Facultad de Ingeniería

Artículo de Investigación (evaluado por pares)

Power Conversion System for Hybrid Battery-Capacitor Storage

Conversión de Potencia para un Sistema de Almacenamiento Híbrido Batería-Capacitor

Carlos Andrés Ramos-Paja

Sergio Ignacio Serna-Garcés

Daniel González-Montoya

Como citar este artículo: C. A. Ramos-Paja, S. I. Serna-Garcés, D. González-Montoya, "Power Conversion System for Hybrid Battery-Capacitor Storage", Ingeniería, Vol. 25, Num. 2, (2020). DOI: https://doi.org/10.14483/23448393.15741

Fecha de envío: 2019-12-17
Modificado: 2020-04-06
Fecha de aceptación: 2020-04-27

Editor: Nelson L. Diaz Aldana.

Research

REVISTA Ingeniería

Power Conversion System for Hybrid Battery-Capacitor Storage

Conversión de Potencia para un Sistema de Almacenamiento Híbrido Batería-Capacitor

***Carlos Andrés Ramos-Paja*[1] *, Sergio Ignacio Serna-Garcés*[*,2] *, Daniel González-Montoya*[2]**

[1]Grupo GAUNAL, Facultad de Minas, Universidad Nacional de Colombia, Medellín, Colombia., [2]Grupo AE&CC, Departamento de Electrónica y Telecomunicaciones, Instituto Tecnológico Metropolitano, Medellín, Colombia.

[*]Correspondence email: sergioserna@itm.edu.co

Received: 17-12-2019. Modified: 06-04-2020. Accepted: 27-04-2020

Resumen

Context: Thanks to the low emissions of CO2 generated by electric systems, those solutions have an increased attention from industry and academia. However, the electrical storage systems required in a large amount of applications must to have both high energy and power densities.

Method: To meet those requirements, this paper proposes an active hybrid energy storage system (HESS), which is formed by a battery, i.e. the device with high energy density, and a capacitor, i.e. the device with high power capability. The proposed power system also protects the battery by limiting the current derivative.

Results: Two sliding-mode controllers (SMC) are designed to regulate both the battery current and the load voltage. The design process guarantees the global stability and safe battery operation.

Conclusions: The controller avoids the battery degradation caused by the high-frequency current components since the capacitor assumes those components demanded by the load profile.

Keywords: hybrid electric storage system, battery, capacitor, sliding-mode controller, Boost converter, Buck converter.

Acknowledgements: Universidad Nacional de Colombia sede Medellín, Instituto Tecnológico Metropolitano, Minciencias.

Language: English.

Resumen

Contexto: Gracias a las bajas emisiones de CO2 de los sistemas eléctricos, estos han ganado mucha atención por parte de la industria y la academia. Sin embargo, los sistemas de almacenamiento de energía requeridos en un sin numero de aplicaciones deben garantizar ser de alta densidad de energía y potencia.

Método: Para satisfacer estos requerimientos, este trabajo propone un sistema de almacenamiento de energía híbrido (HESS) activo, el cual es formado por una batería como dispositivo de alta densidad de energía, y un capacitor como el dispositivo de alta densidad de potencia. Asimismo, la solución propuesta protege la baterí a través de la limitación de la derivada de la corriente.

Resultados: Se diseñan dos controladores por modos deslizantes, uno para la corriente de la batería y otro para regular el voltaje en la carga. El proceso de diseño garantiza la estabilidad global del sistema y una operación segura de la batería.

Conclusiones: El controlador de corriente evita la degradación de la batería causada por los componentes de alta frecuencia de la corriente demandados por la carga. Estos componentes de alta frecuencia son asumidos por el capacitor.

Palabras clave: sistema de almacenamiento híbrido, batería, capacitor, controlador por modos deslizantes, convertidor Boost, convertidor Buck.

Agradecimientos: Universidad Nacional de Colombia sede Medellín, Instituto Tecnológico Metropolitano, Minciencias.

Idioma: Inglés.

1. Introduction

Due to global the warming produced in part by fossil fuels [1], the development of alternative electrical systems has been increased significantly, e.g. public transportation [2]. One of the main challenges of those systems is the power conversion of hybrid energy storage systems - HESS, namely, a system formed by a battery and a capacitor (or a supercapacitor) or a fuel-cell. The main objective of the HESS is to reduce the high-frequency current transients reaching the battery to avoid accelerated aging [3]. Such a purpose is fulfilled by extracting (or storing) the high-frequency components of the load current in a capacitor, hence the battery provides (or stores) the low-frequency components of the current.

Several works have been developed to deal with the power conversion system for HESS. For example, in [2], [3] are presented multiple topologies for HESS (passive, semi-active and active), but the control strategies of each DC/DC converter are not discussed. Other solution is presented in [4], where a composite energy storage system (CESS) is designed using an interleaved bidirectional DAB converter. The control strategy of the DAB converter is based on a proportional current controller for both the battery and the ultracapacitor, hence no global stability is ensured. In [5] a HESS, formed by a battery and a lithium-ion capacitor (LiC), is used for protecting the battery from damages caused by high-power rates during charging and discharging of an urban public transportation. However, such a HESS has a low-complex current controller for the LiC that is not specified. Similarly, an active HESS for domestic applications is proposed in [6], which consist of a battery and a supercapacitor. Both devices have PI-type controllers; one for battery current control, and another one for DC-bus voltage control, but the linearization required for the controller design prevents a global stability proof. A similar approach is reported in [7], which proposes the use of PI-type controller for a three-level bidirectional converter, which together with another

unidirectional converter, manages the power of a HESS formed by a battery and a fuel-cell. Another approach is reported in [8], where a supercapacitor is used to store the energy generated by a manual mechanical system to charge a battery.

A particular approach for designing and controlling HESS concerns the connection of power converters in parallel or series structures. For example, the work reported in [9] presents a HESS for an electrical vehicle, which is formed by a battery and a capacitor interfaced by bidirectional boost converters. Such an approach provides continuous current to the battery due to the series inductor, but it injects discontinuous current to the dc bus, thus degrading the power quality (high ripple current components). This solution has two main problems: first, the load of the HESS is modeled using a constant impedance, which is not accurate to model a dc bus; second, despite the dc bus is regulated, no restriction is imposed to the battery current derivative, which could reduce the battery lifetime [10], [11]. In addition, the converters are controlled with two sliding-mode controllers (SMC) to ensure global stability, which is demonstrated independently for each converter. A similar approach is proposed in [12], where a capacitor and a battery are used to form a HESS. Both devices are interfaced with bidirectional boost converters, hence high current ripple reaches the dc bus. The control systems for both converters are cascade structures of PI-controllers, hence no global stability is ensured. Moreover, no limitation of the battery current derivative is considered. The use of converters with continuous output currents is used to provide low harmonic distortion to the dc bus, which is the case of the battery charger proposed in [13]. In that work, which does not presents a HESS, a bidirectional buck converter is adopted to interface a generic ESS, but at the price of high current ripples to the battery (ESS), which reduces the battery lifetime [10], [11]. The first-level controller of the converter is based on a current controller for a renewable energy source (RES) and a voltage controller for the ESS, but no limitation to the ESS current is provided. The same approach is presented in [14], where a bidirectional buck converter is used to interface a battery avoiding currents with high current ripples. However, the converter controller is based on two cascade PI controllers, and without accounting for any limitation of the battery current derivative.

A simpler approach is presented in [15], [16], where HESS formed by a capacitor and a battery are proposed. However, in those works the only one of the storage devices is interfaced using a dc/dc converter, therefore only one storage device can be controlled. This structure avoids the possibility of decoupling the high-frequency components of the load current from the battery since no limitation in the current derivative is adopted. Moreover, the control systems are, as in the previous cases, cascade structures of PI controllers, which are not able to provide global stability. Therefore, other works such as [17], [18] propose parallel structured based on a battery and a capacitor interfaced with dc/dc converters, which enable to decouple the battery dynamics from the dc bus perturbations. However, in [17] both devices are interfaced with boost converters, hence high current ripples are injected into the dc bus; moreover, both converters are controlled using PI structures, but the design of those controllers is not described. Instead, the work reported in [18] does not report the converters topology, also the controllers design is not discussed. In any case, that work emphasizes the use of a capacitor to provide the high frequency components of the bus current, which is needed to avoid the degradation of the battery lifetime. In addition, both works are intended for electric vehicles, where the speed and lifetime of the storage device is critical.

More advanced control strategies, such as the SMC, have been used to regulate the parallel structures battery/capacitor used to form HESS. For example, the work reported in [19] presents a parallel connection of boost converters to interface a battery and a capacitor with the dc bus, where

both converters are controlled using PI and SMC controllers. The study shows that the SMC provides better performance and an improved stability; however, no limitation in the derivative of the battery current is adopted. Similarly, the work reported in [20] uses a SMC to control the boost converter interfacing the battery, but with two problems: there is not considered any limitation on the current derivative of the battery, and the load is modeled with a constant impedance, which is not an accurate representation of a dc bus. Other work based on sliding-mode theory is reported in [21], which proposes a battery/capacitor HESS based on bidirectional buck converters, hence discontinuous current is injected into the dc bus (high current ripple). The SMC are designed to control the inductor currents, where a cascade voltage controller regulates the bus voltage and a cascade power controller ensures a correct power balance. Finally, the controllers stability is analyzed independently, hence the whole system is stable. The main problem of this work is the absence of a limitation on the battery current derivative to avoid accelerated aging due to high-frequency current transients.

Therefore, to provide a stable dc bus voltage, and to protect the battery from high frequency current transients that could reduce the battery lifetime, this paper proposes a power conversion system for HESS based on bidirectional boost and buck converters. This new power system is designed to provide continuous current to both the battery and the dc bus, and the SMC is adopted to ensure fast response and global stability. The remain of the paper is organized as follow: the active topology proposed for the HESS is presented in Section 2, then the design of the sliding-mode controllers for each converter, guaranteeing the global stability of the system, is presented in Section 3. Section 4 reports an application example and the system simulations for a case of study. Finally, the conclusions close the paper.

2. Electrical structure of the power conversion system

The main objective of the proposed solution is to reduce the high frequency current transients reaching the battery. Such an objective is fulfilled by extracting (or storing) the high frequency components of the load current in a capacitor, hence the battery provides (or stores) the low frequency components of the current.

Fig. 1 presents the circuital scheme of the proposed power conversion system, where the voltage source v_b represents the battery and C_b represents the auxiliary storage capacitor. The battery is isolated from the load by means of a boost converter, while the capacitor is isolated using a buck converter. The boost converter is used to interface the battery since it imposes continuous current to the battery, hence avoiding high current transients. Instead, the buck converter is selected to interface the capacitor due to the continuous current provided at the output, which corresponds to an additional voltage regulation capacitor C_{dc}. This last condition makes possible to regulate the voltage of C_{dc} to provide a regulated voltage level to the load in any condition: discharge mode (positive battery current), charge mode (negative battery current) and stand-by mode (null battery current).

The boost converter has a bi-directional structure (replacing the diode with a MOSFET) with an inductor L_b that imposes the battery current ($i_{Lb} = i_b$). The buck converter also has a bi-directional structure with an inductor L_c (i_{Lc} current). The voltage of the output capacitor C_{dc} is perturbed by the output current of the boost converter (i_{bo}), the inductor current of the buck converter (i_{Lc}) and the load current (i_{dc}). Therefore, i_{Lc} current must be controlled to provide a regulated output

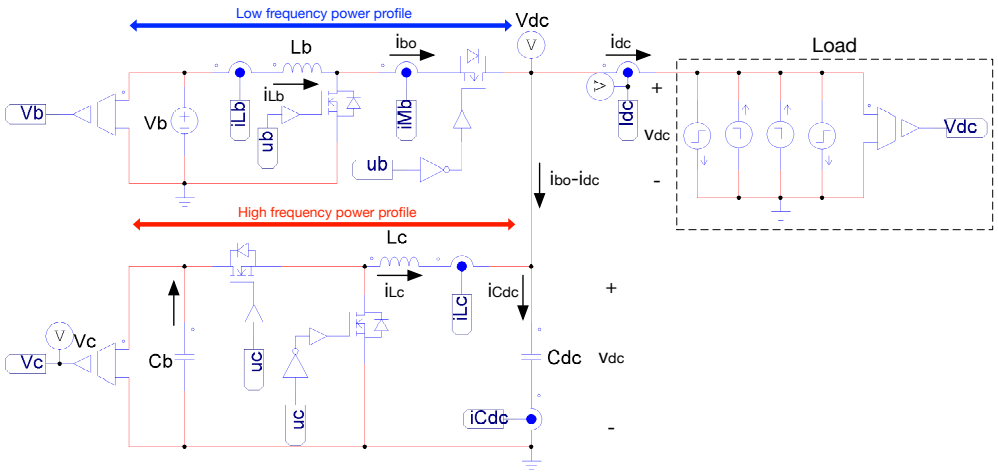

Figura 1. Electrical scheme of the proposed power conversion system for hybrid battery-capacitor storage.

voltage v_{dc}, while the battery current i_{Lb} must be regulated to limit the current derivative within safe limits, which in turns protects the battery from high-frequency currents.

The circuital scheme represents the load with current steps, which corresponds to the current profiles with highest derivative, both positive and negative. Finally, the proposed power conversion system provides a regulated voltage to the load in any operation condition, hence behaving as an ideal voltage source.

3. Sliding-mode controllers

In order to regulate both the battery current and the load voltage, two sliding-mode controllers (SMC) are designed. The first one is in charge of regulating the i_{Lb} current, hence imposing a safe profile to the battery current; the second controller is in charge of regulating the load voltage v_{dc}. In the following, the mathematical model of the circuit and both SMC are described.

3.1. Mathematical model

The differential equations modeling the inductors currents and capacitors voltages are:

$$\frac{di_{Lb}}{dt} = \frac{v_b - v_{dc} \cdot (1 - u_b)}{L_b} \tag{1}$$

$$\frac{di_{Lc}}{dt} = \frac{v_c \cdot u_c - v_{dc}}{L_c} \tag{2}$$

$$\frac{dv_{dc}}{dt} = \frac{i_{Lc} - i_{dc} + i_{bo}}{C_{dc}} \tag{3}$$

$$\frac{dv_c}{dt} = \frac{-i_{Lc} \cdot u_c}{L_b} \tag{4}$$

In those equations u_b represents the control signal driving the MOSFETs of the boost converter, while u_c represents the signal driving the MOSFETs of the buck converter. Moreover, averaging

those equations within the switching period [22], the average values of the output current in the boost converter i_{bo} and its duty cycle d_b are:

$$i_{bo} = i_{Lb} \cdot (1 - d_b) \tag{5}$$

$$d_b = 1 - \frac{v_b}{v_{dc}} \tag{6}$$

3.2. Sliding-mode controllers

The objective of this SMC is to regulate the L_b current (i_{Lb}) in agreement with a given reference value i_{br}. Such a behavior is obtained by imposing the following switching function S_b with the sliding surface $S_b = 0$:

$$S_b = i_{br} - i_{Lb} \tag{7}$$

The derivative of the previous switching function is:

$$\frac{dS_b}{dt} = \frac{di_{br}}{dt} - \frac{v_b - v_{dc} \cdot (1 - u_b)}{L_b} \tag{8}$$

The global stability of a SMC for switched power converters is evaluated using the three conditions described in [23]: transversality, reachability and equivalent control. Moreover, Sira-Ramirez in [24] demonstrated that both reachability and equivalent control conditions are equivalent, hence only one of them must be evaluated. Therefore, any SMC that fulfills both transversality and reachability conditions is globally stable.

3.2.1. Transversality condition

The transversality condition evaluates the presence of the control signal into the derivative of the switching function [25], hence it evaluates the controlability of the system:

$$\frac{d}{du_b}\left(\frac{dS_b}{dt}\right) \neq 0 \tag{9}$$

Replacing (8) into (9):

$$\frac{d}{du_b}\left(\frac{dS_b}{dt}\right) = -\frac{v_{dc}}{L_b} < 0 \tag{10}$$

Since (10) is true in any condition, the transversality condition is always fulfilled. Therefore, it is possible to implement a SMC based on the sliding surface $S_b = 0$.

3.2.2. Reachability condition

The reachability conditions analyze the convergence of the switching function S_b to the sliding surface $S_b = 0$ [25]. In that way, when S_b is operating under the surface, the derivative of S_b must be positive to reach the surface; similarly, when S_b is operating above the surface, the derivative of S_b must be negative to reach the surface. The previous conditions are formalized as follow:

$$\lim_{S_b \to 0^-} \frac{dS_b}{dt} > 0 \ \wedge \ \lim_{S_b \to 0^+} \frac{dS_b}{dt} < 0 \tag{11}$$

The analysis of (11) depends on the sign of the transversality condition (10). Since $\frac{d}{du_b}\left(\frac{dS_b}{dt}\right) < 0$, it means that a positive change in u_b produces a negative S_b derivative, while a negative change in u_b produces a positive S_b derivative. Therefore, to achieve $\frac{dS_b}{dt} > 0$ it is needed that u_b changes to 0, and to achieve $\frac{dS_b}{dt} < 0$ it is needed that u_b changes to 1. Then, using the value of S_b given in (8) to evaluate (11), the following reachability conditions are obtained:

$$\lim_{S_b \to 0^-} \left.\frac{dS_b}{dt}\right|_{u_b=0} = \frac{di_{br}}{dt} - \frac{v_b - v_{dc}}{L_b} > 0 \tag{12}$$

$$\lim_{S_b \to 0^+} \left.\frac{dS_b}{dt}\right|_{u_b=1} = \frac{di_{br}}{dt} - \frac{v_b}{L_b} < 0 \tag{13}$$

Both inequalities (12) and (13) impose dynamic restrictions to the reference i_{br}, which is used to define the battery current. The practical dynamic restrictions are given in (14), which must be fulfilled to guarantee reaching the sliding surface.

$$\frac{v_b - v_{dc}}{L_b} < \frac{di_{br}}{dt} < \frac{v_b}{L_b} \tag{14}$$

Analyzing the L_b current derivative given in (1), it is concluded that the limits of inequality (14) corresponds to the maximum positive and negative derivatives of L_b current, hence the proposed SMC based on S_b enables to reach the fastest response possible for the boost converter.

Finally, since both transversality and reachability conditions are fulfilled, the analyses reported in [24] ensure that the dc/dc converter controlled by the proposed SMC has global stability.

3.2.3. Reference generator

The reference for the battery current i_{br} must be defined following two conditions:

- The derivative of i_{br} must fulfill restrictions given in (12).
- The average battery power $p_b = v_b \cdot i_{br}$ must be equal to the average load power $p_{dc} = v_{dc} \cdot i_{dc}$. In that way the average power exchanged with the capacitor is zero, hence it has a constant average charge.

The previous conditions are fulfilled using the structure depicted in Fig. 2, which also presents the flowchart of the power balance algorithm. First, the theoretical battery current i^*_{br} needed to balance the capacitor power is calculated as $i^*_{br} = v_{dc} \cdot \frac{i_{dc}}{v_b}$, which could exhibit high frequency components; therefore, a circuit limiting the derivative of i^*_{br} signal is introduced. Such a derivative limiter is configured to ensure a maximum current derivative lower than the safe slew-rate value SR, which depends on the battery specifications. Finally, the reference current i_{br} corresponds to the output of the derivative limiter.

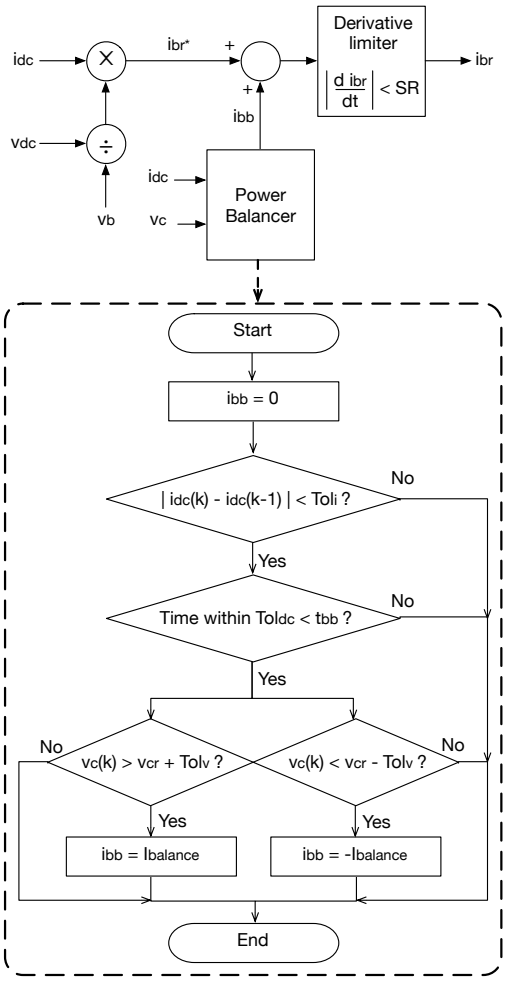

Figura 2. i_{br} reference generator structure and power balance algorithm.

Second, since the high frequency current transients are not provided in i_{br}, the capacitor charge is not balanced after a high frequency transient. To balance the capacitor charge, an additional power balance algorithm is used: this algorithm increases or decreases the i_{br} reference, using the signal i_{bb}, until the capacitor voltage reaches a reference value v_{cr} within an acceptable tolerance Tol_v. This hysteretic tolerance is introduced to avoid voltage chattering around v_{cr}. Moreover, the power balance block is active when the load current is stable within a tolerance band Tol_i, i.e. without high frequency transients: to activate the power balance block, the changes of the load current i_{dc} must be within the tolerance band Tol_i during at least t_{bb} seconds. When those conditions are fulfilled, the signal i_{bb} is equal to a safe current magnitude $I_{balance}$ used to balance the capacitor as follow:

if the capacitor voltage is under the hysteresis band $v_{cr} - Tol_v$, then $i_{bb} = I_{balance}$; if the capacitor voltage is over the hysteresis band $v_{cr} + Tol_v$, then $i_{bb} = -I_{balance}$; otherwise $i_{bb} = 0$.

In conclusion, the power balance block only acts when the load current is stable for a predefined time interval.

3.2.4. Controller implementation

The implementation of the SMC based on S_b must be done using a hysteresis comparator to limit the switching frequency [26]. Such an implementation is performed by imposing a control law in agreement with the reachability conditions (12) and (13), but including the hysteresis band ($-H_b$, $+H_b$) as it is given in (15). Therefore, the practical sliding surface becomes $-H_b \leq S_b \leq +H_b$; and the controller is stable if the switching function always operates inside hysteresis band.

$$\begin{cases} \text{if } S_b < -H_b \rightarrow u_b = 0 \\ \text{if } S_b > +H_b \rightarrow u_b = 1 \end{cases} \tag{15}$$

The previous control law is implemented using two classical comparators and Flip-Flop S-R. The circuital implementation of such a control law is presented in Fig. 3, which also depicts the implementation of the derivative limiter (SR) and the power balance block. The algorithm of that block was coded in C language. Finally, the hysteresis band H_b is selected to limit the switching frequency below a practical value.

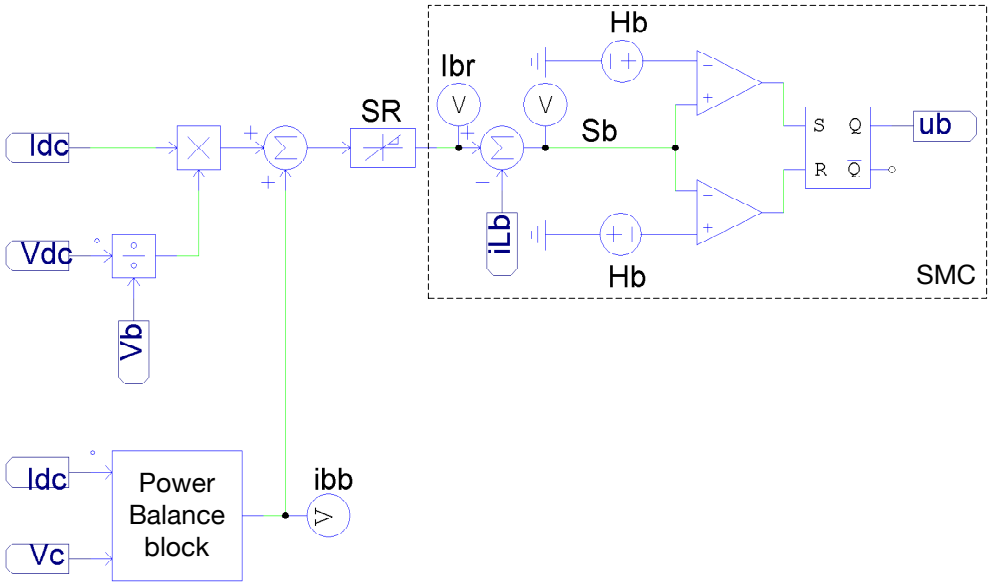

Figura 3. SMC based on S_b.

3.3. Sliding-mode controller for the output voltage

The objective of this SMC is to regulate the L_c current (i_{Lc}) following a reference value i_{cr} generated by a voltage controller, which in turns must to provide a regulated output voltage v_{dc}. This SMC is based on the following switching function S_c with the sliding surface $S_c = 0$:

$$S_c = i_{cr} - i_{Lc} \tag{16}$$

The derivative of the previous switching function is:

$$\frac{dS_c}{dt} = \frac{di_{cr}}{dt} - \frac{v_c \cdot u_c - v_{dc}}{L_c} \tag{17}$$

3.3.1. Transversality condition

The transversality condition of this part of the system is:

$$\frac{d}{du_c}\left(\frac{dS_c}{dt}\right) \neq 0 \tag{18}$$

Replacing (17) into (18):

$$\frac{d}{du_c}\left(\frac{dS_c}{dt}\right) = -\frac{v_c}{L_c} < 0 \tag{19}$$

Since (19) is always true, hence the transversality condition is always fulfilled. Therefore, it is possible to implement a SMC based on the sliding surface $S_c = 0$.

3.3.2. Reachability conditions

Taking into account that the transversality value (19) is negative, the reachability conditions are similar to the ones obtained for the previous SMC:

$$\lim_{S_c \to 0^-} \left.\frac{dS_c}{dt}\right|_{u_c=0} = \frac{di_{cr}}{dt} + \frac{v_c}{L_c} > 0 \tag{20}$$

$$\lim_{S_c \to 0^+} \left.\frac{dS_c}{dt}\right|_{u_c=1} = \frac{di_{cr}}{dt} - \frac{v_c - v_{dc}}{L_c} < 0 \tag{21}$$

The previous inequalities impose the following dynamic restrictions to the reference i_{cr}:

$$-\frac{v_{dc}}{L_c} < \frac{di_{cr}}{dt} < \frac{v_c - v_{dc}}{L_c} \tag{22}$$

As in the previous SMC, the L_c current derivative given in (2) shows that the limits of inequality (22) correspond to the maximum positive and negative derivatives of L_c current, hence the reachability conditions are always fulfilled. Moreover, such an expression also puts into evidence that the SMC based on S_c enables to reach the fastest response possible for the buck converter.

Finally, as in the previous SMC, since both transversality and reachability conditions are fulfilled, the analyses reported in [24] ensure that the buck converter controlled by this SMC has global stability.

3.3.3. Equivalent dynamics of the SMC

The action of the SMC based S_c over the buck converter (high frequency power profile in Fig. 1) enables to impose a desired current profile i_{cr} in L_c. Therefore, L_c could be modeled as a controlled current source with value i_{cr}. Moreover, in steady-state conditions the battery must to provide (or store) the load current, hence the steady-state value of i_{cr} is zero. The previous conditions imply that a change δi_{dc} in the load current is equal to the difference between the new load current (after the perturbation) and the steady-state current at the output of the boost converter I_{bo}. In mathematical terms, the load current after perturbations is given by (23), where I_{dc} is the steady-state current of the load (previous to the perturbation). Finally, the load current perturbation is calculated in (24) as the difference between the load current and the steady-state current at the output of the boost converter I_{bo}.

$$i_{dc} = \delta i_{dc} + I_{dc} \tag{23}$$

$$\delta i_{dc} = i_{dc} - I_{bo} \tag{24}$$

From the circuit depicted in Fig. 1, and from eqs. (3), (5) and (24), the output capacitor current is:

$$i_{Cdc} = i_{cr} - \delta i_{dc} = C_{dc} \cdot \frac{dv_{dc}}{dt} \tag{25}$$

Applying the Laplace transformation to eq. (25):

$$v_{dc}(s) = \frac{i_{cr}(s)}{s \cdot C_{dc}} - \frac{\delta i_{dc}(s)}{s \cdot C_{dc}} \tag{26}$$

The block diagram of the equivalent system is depicted in Fig. 4, which includes the reference value v_r for the load voltage and an additional controller $G_v(s)$ for defining the reference i_{cr} of the SMC. This paper proposes to implement $G_v(s)$ using a fixed gain k_p, which produces the following closed-loop dynamics:

$$\frac{v_{dc}(s)}{v_r(s)} = \frac{1}{\frac{C_{dc}}{k_p} \cdot s + 1} \tag{27}$$

Therefore, k_p is designed using (28) to impose a desired settling time t_s to the load voltage.

$$k_p = \frac{4 \cdot C_{dc}}{t_s} > 0 \tag{28}$$

Equations (27) and (28) put into evidence the stability of the bus voltage: k_p and C_{dc} always have positive values, hence the equivalent closed-loop pole of (27) is located at $s = -\frac{k_p}{C_{dc}} < 0$, which ensures a global stability of the bus voltage.

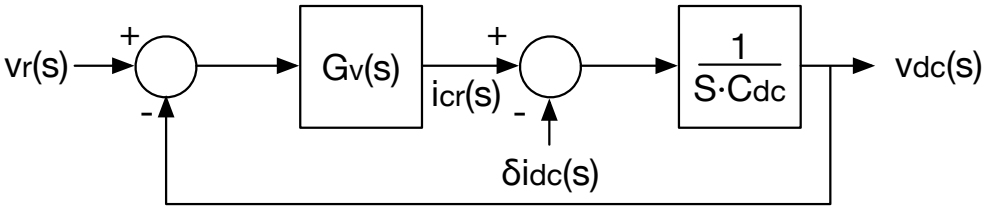

Figura 4. Equivalent system of S_c.

3.3.4. Controller implementation

Similar to the implementation of the previous controller, the SMC based on S_c must be implemented using a hysteresis comparator to limit the switching frequency [26]. In this case the control law is in agreement with the reachability conditions (20) and (21) including the hysteresis band ($-H_c$, $+H_c$) as it is given in (29). Therefore, the practical sliding surface becomes $-H_c \leq S_c \leq +H_c$; and the controller is stable if the switching function always operates inside hysteresis band.

$$\begin{cases} \text{if } S_c < -H_c \rightarrow u_c = 0 \\ \text{if } S_c > +H_c \rightarrow u_c = 1 \end{cases} \tag{29}$$

Such a control law is implemented using two classical comparators and Flip-Flop S-R. Fig. 5 presents the circuital implementation, where the hysteresis band H_c is selected to limit the switching frequency below a practical value.

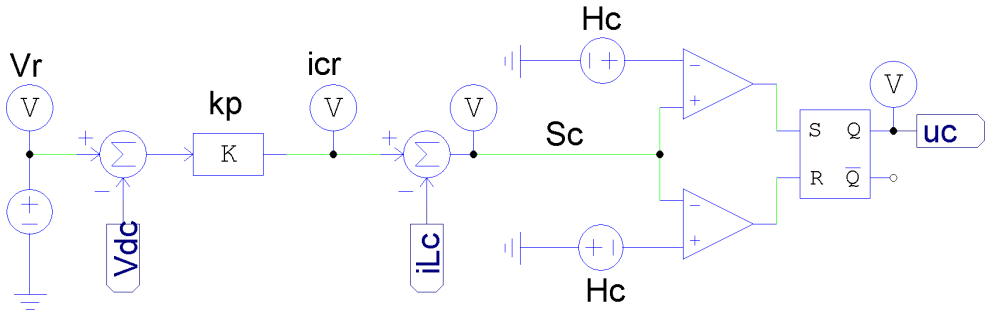

Figura 5. SMC based on S_c.

4. Design example and circuital simulations

To illustrate the system design and performance, the parameters given in Table I are considered, where the hysteresis bands were selected to limit the switching frequencies up to 200 kHz. Finally, the controller parameter $k_p = 1{,}333$ was calculated from (28) to impose a settling time equal to $0{,}3$ ms.

Fig. 6 presents the behavior of the power system for fast current transients in the load current: it is observed that both positive and negative currents are imposed by the load, but in all cases the load voltage is successfully regulated. Moreover, the limitation of the slew-rate of the battery current is also observed, which also corresponds to the current of the inductor L_b. Therefore, the

Cuadro I. Simulation parameters

Parameter	Value
Battery voltage	$v_b = 12\ V$
Maximum slew-rate for the battery current	$S_r = 10\ A/ms$
Boost converter inductance	$L_b = 100\ \mu H$
Hysteresis band for the boost	$H_b = 0{,}3$
Storage capacitor	$C_b = 100\ \mu F$
Storage capacitor reference	$v_{cr} = 48\ V$
Buck converter inductance	$L_c = 100\ \mu H$
Hysteresis band for the buck	$H_c = 0{,}28$
Bus capacitor	$C_{dc} = 100\ \mu F$
Bus voltage reference	$v_r = 24\ V$
Desired settling time for the bus voltage	$t_s = 0{,}3\ ms$

proposed solution is effective in any operation condition: charging the battery, discharging the battery, and without energy exchange with the battery (stand-by mode). Fig. 7 present different phase planes of the power system for the simulation presented in Fig. 6. Fig. 7(a) shows the phase plane for the buck converter, which regulates the bus voltage: it is observed that the bus voltage is around the reference value independent of the inductor current i_{L_C}, which could be positive (discharge), negative (charge) or zero (stand-by). Fig. 7(b) shows the switching function S_c of the buck converter, which always operates into the hysteresis band $-H_c \leq S_c \leq +H_c$, hence the sliding-mode exists and the system is globally stable. Fig. 7(c) presents the phase plane of the boost converter, where the battery current (buck inductor current) follows with null error the current reference in any condition, i.e. discharge (positive), charge (negative) or stand-by (zero). Finally, Fig. 7(d) shows the switching function S_b of the boost converter, which also operates into the hysteresis band $-H_b \leq S_b \leq +H_b$, hence the sliding-mode exists and the closed-loop boost converter is globally stable.

Fig. 8 presents the simulation of two consecutive current transients, which increases the current load, and after the second perturbation the load current remains constant (equal to $2\ A$). The simulation shows that both perturbations reduce the C_b capacitor voltage, since such a capacitor is in charge of delivering the high frequency components of the transient. In this example the power balance block was configured to start the compensation after $t_{bb} = 2\ ms$ of stable conditions, introducing a compensation current $i_{bb} = 250\ mA$, but any other values can be used depending on the particular application. The simulation of Fig. 8 shows that the power balance block increases the inductor current of the boost converter in $250\ mA$, over the current requested by the load, to charge the capacitor. In fact, when the capacitor voltage is restored to $v_{cr} = 48\ V$, the compensation current i_{bb} is set to $0\ A$.

Fig. 9(a) shows the phase plane for the buck converter for this simulation, where the bus voltage is regulated around the reference value for any inductor current i_{L_C} value, e.g. positive (discharge), negative (charge) or zero (stand-by). Fig. 9(b) shows the switching function S_c of the buck converter for this simulation, which also operates into the hysteresis band $-H_c \leq S_c \leq +H_c$, hence the sliding-mode exists and the buck converter is globally stable. Similarly, Fig. 9(d) shows the switching function S_b of the boost converter, which also operates into the hysteresis band $-H_b \leq S_b \leq +H_b$, and the boost converter is globally stable. Finally, Fig. 9(c) presents the

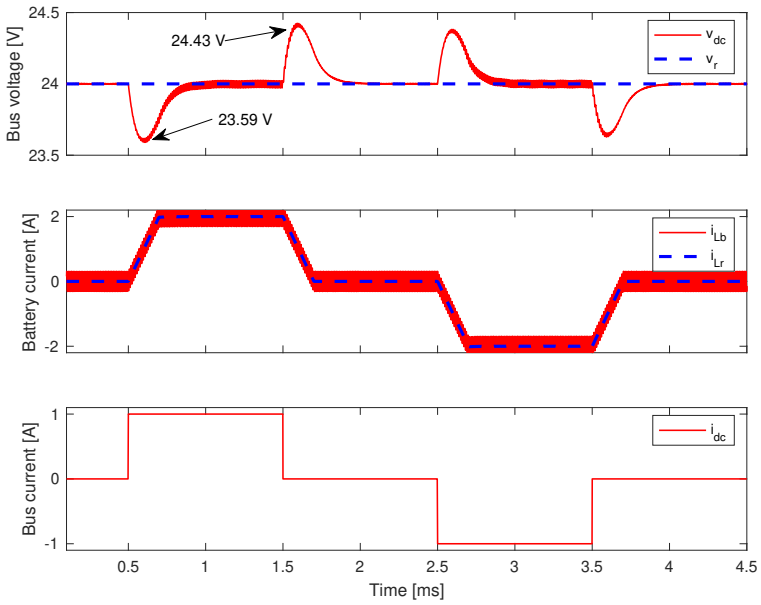

Figura 6. Simulation of the power system under fast load perturbations.

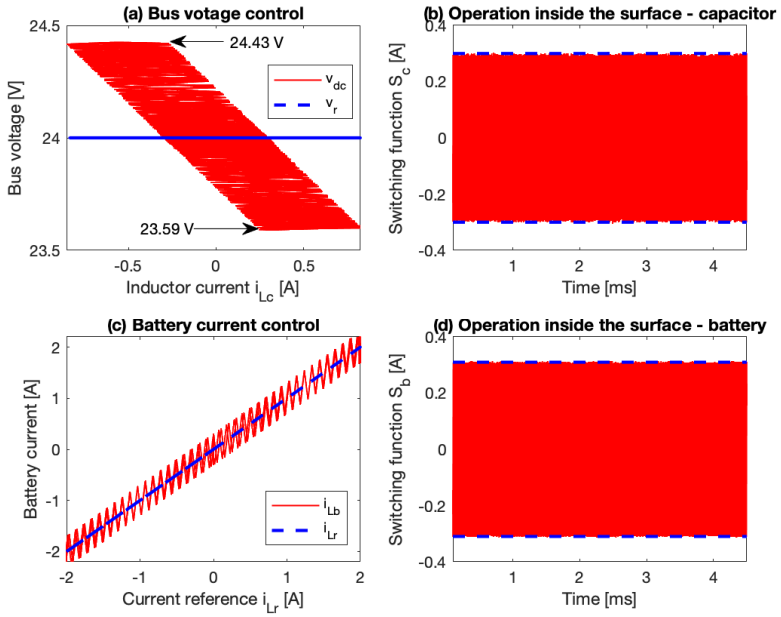

Figura 7. Phase planes of the power system under fast load perturbations.

phase plane of the buck converter in terms of the storage capacitor voltage, which is regulated by the power balance block around the reference value for any condition of the inductor current, i.e. discharge (positive), charge (negative) or stand-by (zero).

In conclusion, the simulations presented in this section put into evidence the correct behavior of the proposed solution:

- The load voltage is regulated in any operation condition.

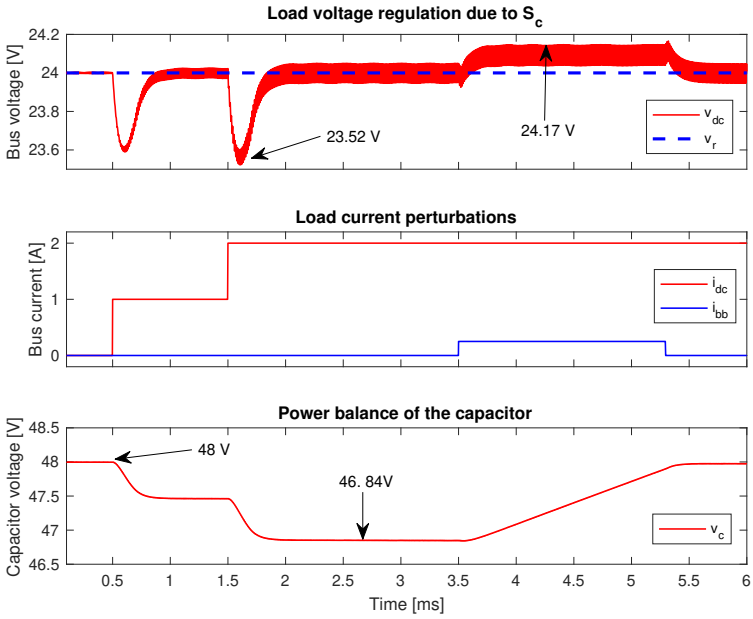

Figura 8. Action of the power balance block.

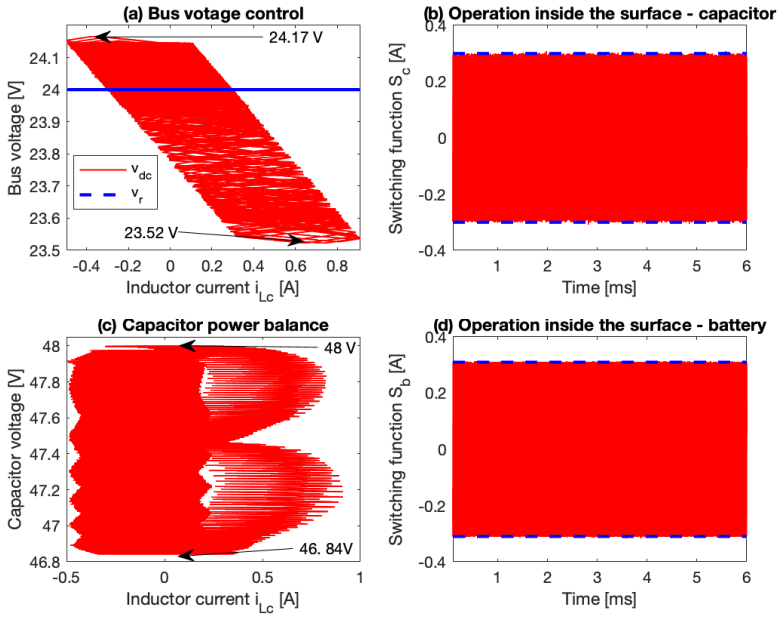

Figura 9. Phase planes of the system under the action of the power balance block.

- The battery is not exposed to high frequency currents.
- The auxiliary capacitor charge is balanced.
- Both SMC exhibit global stability.

5. Conclusions

This paper reports an active HESS formed by a battery, a capacitor and two dc/dc converters. Two sliding-mode controllers were designed, one for a Boost converter and another for a Buck converter. The Boost converter interfaces the battery with the load, and it is controlled to avoid injecting high-frequency transients into the battery. The second controller operates on the Buck converter that isolates the capacitor of the load. This SMC acts on the converter to provide a regulated voltage to the load in any condition. Moreover, the existence of both sliding surfaces is guaranteed, which confirms the global stability of the system.

The simulation results show a performance of both the bus voltage regulation and battery current regulation fulfilling the design criteria. The results also show that the load voltage is regulated in any operation condition, the battery is not exposed to high-frequency currents, and the auxiliary capacitor charge is balanced.

The main limitation of this solution concerns the use of a loss-less energy balance for the regulation of the steady-state value of the battery current. This limitation could be addressed, in a future work, by including additional current sensors to the circuit, accounting for parasitic losses, but at the price of increasing the system cost. The experimental verification of this solution is under development, which will account for the previous limitation. Finally, a future improvement could consider the adoption of step up/down high-order converters to enable the connection of any battery to any bus voltage level, e.g. buck-boost converters with input/output filters, Cuk, Sepic or Zeta converters, among others.

Acknowledgments

This work was supported by the Instituto Tecnológico Metropolitano (Project P17211), the Universidad Nacional de Colombia and Minciencias (Fondo nacional de financiamiento para ciencia, la tecnología y la innovación Francisco José de Caldas) under the projects “Estrategia de transformación del sector energético Colombiano en el horizonte de 2030 - Energetica 2030”, and “Generación distribuida de energía eléctrica en Colombia a partir de energía solar y eólica”(Code: 58838, Hermes: 38945).

Referencias

[1] M. Hoel and S. Kverndokk, “Depletion of fossil fuels and the impacts of global warming,” *Resource and Energy Economics*, vol. 18, no. 2, pp. 115–136, jun 1996.

[2] T. Zimmermann, P. Keil, M. Hofmann, M. F. Horsche, S. Pichlmaier, and A. Jossen, “Review of system topologies for hybrid electrical energy storage systems,” *Journal of Energy Storage*, vol. 8, pp. 78–90, nov 2016.

[3] J. Cao and A. Emadi, “A New Battery/UltraCapacitor Hybrid Energy Storage System for Electric, Hybrid, and Plug-In Hybrid Electric Vehicles,” *IEEE Transactions on Power Electronics*, vol. 27, no. 1, pp. 122–132, jan 2012.

[4] H. Zhou, T. Bhattacharya, D. Tran, T. S. T. Siew, and A. M. Khambadkone, “Composite Energy Storage System Involving Battery and Ultracapacitor With Dynamic Energy Management in Microgrid Applications,” *IEEE Transactions on Power Electronics*, vol. 26, no. 3, pp. 923–930, mar 2011.

[5] M. Soltani, J. Ronsmans, S. Kakihara, J. Jaguemont, P. Van den Bossche, J. van Mierlo, and N. Omar, “Hybrid Battery/Lithium-Ion Capacitor Energy Storage System for a Pure Electric Bus for an Urban Transportation Application,” *Applied Sciences*, vol. 8, no. 7, p. 1176, jul 2018.

[6] X. Wang, D. Yu, S. Le Blond, Z. Zhao, and P. Wilson, "A novel controller of a battery-supercapacitor hybrid energy storage system for domestic applications," *Energy and Buildings*, vol. 141, pp. 167–174, apr 2017.
[7] K. Jin, M. Yang, X. Ruan, and M. Xu, "Three-Level Bidirectional Converter for Fuel-Cell/Battery Hybrid Power System," *IEEE Transactions on Industrial Electronics*, vol. 57, no. 6, pp. 1976–1986, jun 2010.
[8] J. S. Vanegas Varon, M. A. Latorre González, and J. D. Rairán Antoniles, "Cargador manual de baterías: prototipo académico," *Revista Ingeniería*, vol. 21, no. 1, pp. 83–95, 2016.
[9] "Applications of battery/supercapacitor hybrid energy storage systems for electric vehicles using perturbation observer based robust control," *Journal of Power Sources*, vol. 448, p. 227444, 2020.
[10] J. Li, A. M. Gee, M. Zhang, and W. Yuan, "Analysis of battery lifetime extension in a smes-battery hybrid energy storage system using a novel battery lifetime model," *Energy*, vol. 86, pp. 175 – 185, 2015.
[11] G. Ning, B. Haran, and B. N. Popov, "Capacity fade study of lithium-ion batteries cycled at high discharge rates," *Journal of Power Sources*, vol. 117, no. 1, pp. 160 – 169, 2003.
[12] E. A. Narvaez, C. A. C. Guerrero, and C. L. T. Rodriguez, "Topologies for battery and supercapacitor interconnection in residential microgrids with intermittent generation," *Ingenieria*, vol. 25, no. 1, pp. 1 – 11, 2020.
[13] R. Han, M. Tucci, A. Martinelli, J. M. Guerrero, and G. Ferrari-Trecate, "Stability analysis of primary plug-and-play and secondary leader-based controllers for dc microgrid clusters," *IEEE Transactions on Power Systems*, vol. 34, no. 3, pp. 1780–1800, 2019.
[14] S. Najafi-Shad, S. M. Barakati, and A. Yazdani, "An effective hybrid wind-photovoltaic system including battery energy storage with reducing control loops and omitting pv converter," *Journal of Energy Storage*, vol. 27, p. 101088, 2020.
[15] O. Veneri, C. Capasso, and S. Patalano, "Experimental investigation into the effectiveness of a super-capacitor based hybrid energy storage system for urban commercial vehicles," *Applied Energy*, vol. 227, pp. 312 – 323, 2018.
[16] L. Sun, P. Walker, K. Feng, and N. Zhang, "Multi-objective component sizing for a battery-supercapacitor power supply considering the use of a power converter," *Energy*, vol. 142, pp. 436 – 446, 2018.
[17] M. Sellali, S. Abdeddaim, A. Betka, A. Djerdir, S. Drid, and M. Tiar, "Fuzzy-super twisting control implementation of battery/super capacitor for electric vehicles," *ISA Transactions*, vol. 95, pp. 243 – 253, 2019.
[18] S. Ahmadi, S. Bathaee, and A. H. Hosseinpour, "Improving fuel economy and performance of a fuel-cell hybrid electric vehicle (fuel-cell, battery, and ultra-capacitor) using optimized energy management strategy," *Energy Conversion and Management*, vol. 160, pp. 74 – 84, 2018.
[19] A. Etxeberria, I. Vechiu, H. Camblong, and J.-M. Vinassa, "Comparison of sliding mode and pi control of a hybrid energy storage system in a microgrid application," *Energy Procedia*, vol. 12, pp. 966 – 974, 2011.
[20] B. Wang, J. Xu, D. Xu, and Z. Yan, "Implementation of an estimator-based adaptive sliding mode control strategy for a boost converter based battery/supercapacitor hybrid energy storage system in electric vehicles," *Energy Conversion and Management*, vol. 151, pp. 562 – 572, 2017.
[21] Z. Song, J. Hou, H. Hofmann, J. Li, and M. Ouyang, "Sliding-mode and lyapunov function-based control for battery/supercapacitor hybrid energy storage system used in electric vehicles," *Energy*, vol. 122, pp. 601 – 612, 2017.
[22] D. W. Hart, *Electrónica de Potencia*, 1st ed. Madrid: Pearson Educación, S.A., 2001.
[23] D. González-Montoya, C. A. Ramos-Paja, and R. Giral, "Improved Design of Sliding-Mode Controllers Based on the Requirements of MPPT Techniques," *IEEE Transactions on Power Electronics*, vol. 31, no. 1, pp. 235–247, jan 2016. [Online]. Available: http://ieeexplore.ieee.org/lpdocs/epic03/wrapper.htm?arnumber=7024938
[24] H. Sira-Ramirez, "Sliding motions in bilinear switched networks," *IEEE Transactions on Circuits and Systems*, vol. 34, no. 8, pp. 919–933, aug 1987.
[25] V. I. Utkin, *Sliding Modes in Control and Optimization*. Berlin, Heidelberg: Springer Berlin Heidelberg, 1992.
[26] S. I. Serna-Garcés, "Contributions to the efficiency and safety of stand-alone dc microgrids," 2018.

Carlos Andrés Ramos-Paja

He was born in Cali, Colombia, in 1978. He received the engineer degree in electronics from the Universidad del Valle-Colombia in 2003, a master degree on automatic control from the same university in 2005, and the Ph.D. degree in power electronics from the Universitat Rovira i Virgili-Spain in 2009. Since 2009 he has been Professor in the Universidad Nacional de Colombia, where he is Full Professor. His main research interests are in the design and control of renewable energy systems, switching converters, distributed power systems, and power quality solutions.

Sergio Ignacio Serna-Garcés

He was born in Medellín, Colombia, in 1971. He received the engineer degree in electrical from the Universidad Nacional de Colombia in 1998, and electronics from the Universidad de Antioquia in 2005, a master degree on system engineering from the Universidad Nacional de Colombia in 2011, and the degree of Doctor of Engineering - Automatic Engineering from the same University in 2019. Since 2015 he has been Professor in the Instituto Tecnológico Metropolitano in Medellín-Colombia, where he is Assistant Professor. His main research interests are in DC/DC switching converter design, the design and control of renewable energy systems, and embedded systems.

Daniel González-Montoya

He was born in Medellin, Colombia. He received the engineer degree in control from the Universidad Nacional de Colombia in 2010, a master degree on industrial automatic from the same university in 2012, and the Ph.D. degree in automatic engineering from the Universidad Nacional de Colombia in 2017. Since 2015 he has Professor in the Instituto Tecnologico Metropolitano ITM. His main research interests are in the design control strategies of renewable energy systems and switching converters.